

Oscillating Systems with Elastic Element Moving between Guides with given Shape

Alexei Zotov^{1*}, Anvar Valeev¹, Sergey Glebov¹

Abstract

Oscillations of the systems with force characteristics with hysteresis loops of rectangular shape obtained by dry friction forces are analyzed. Linear and rotary cases of the system were analyzed. Designs of these systems are presented. The analyzed systems can be used in different fields: seismic protection, chassis of transport, exoskeletons.

Keywords

Oscillation, quasi-zero stiffness, vibration protection, impact protection, hysteresis loops, dry friction

¹ Ufa State Petroleum Technological University, Ufa, Russian Federation

* **Corresponding author:** a-zot2@yandex.ru

Introduction

Analyses of damped oscillations of a protected object after the impact for systems with force characteristics with hysteresis loops of rectangular shape obtained by dry friction forces were made. These systems can be used for protection against vibration and impact.

Linear and rotary cases were analyzed. In the linear case only translational movement of the protected object was considered. In rotary case only a rotational movement was analyzed. Analogies of both cases were presented. The coefficients that determine the height of the hysteresis loop in terms of minimizing the time damping after the impact were calculated. Schemes of these systems are presented.

1. Modeling of impact protection by means of systems with force characteristics with rectangular hysteresis loops

Systems with such kind of force characteristics were observed (Fig. 1) [1-4]. Dependences of restoring force $F(x)$ on displacement and restoring moment on angle $M(\varphi)$ are presented on the Fig. 1. Force of dry friction $R = q \cdot F_*$ in linear case or moment of friction $R' = q \cdot M_*$ in rotational case is added, and at the reverse movement is subtracted. Coefficient q describes height of hysteresis loops, $0 \leq q \leq 1$

Impact is simulated by the following way. Let the protected object have the initial velocity V_0 (Fig. 2, a) or the initial angular velocity ω_0 (Fig. 2, b). Damping of the impacted object is provided by the systems with force characteristics shown in Fig. 1.

The differential equation describing motion in the case of force characteristics shown in Fig. 1, is the following (for both translational and rotational movements):

$$a \cdot \ddot{z}(t) + (q \cdot B) \cdot \text{sign}(\dot{z}(t)) + B \cdot \text{sign}(z(t)) = 0, \quad (1)$$

where $a=m$ is the mass of the protected object in a linear case (Fig. 2, a); $a=I_0$ is the moment of inertia relative to the rotational center (Fig. 2, b); $B=F_*$ is the constant restoring force in a linear case (Fig. 1, a, Fig. 2, a); $B=M_*$ is the constant restoring moment in a rotational case (Fig. 1, a, Fig. 2, b); $z=x$ is the displacement of the protected object in a linear case (Fig. 2, a); $z=\varphi$ is the angular displacement of the protected object in a rotational case (Fig. 2, b).

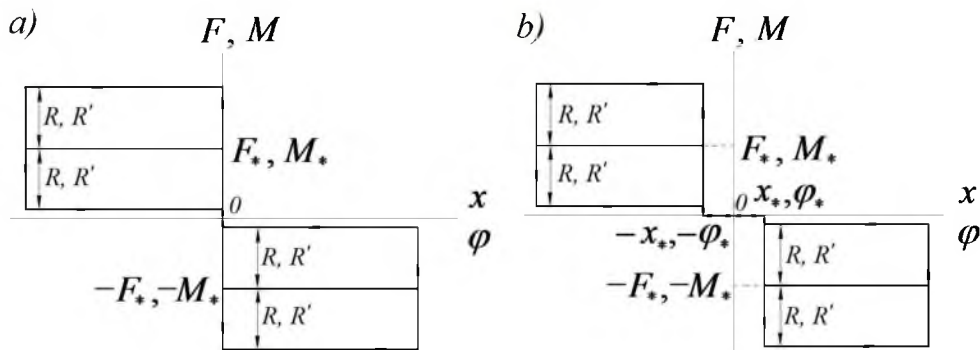


Figure 1. Force characteristics with loops of rectangular shape
 a) Without interval, with zero force and in a neutral position; b) With interval, with zero force and in a neutral position ($F(x)$ – restoring force, $M(\varphi)$ – restoring moment)

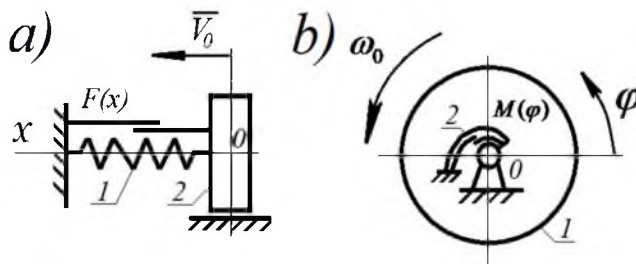
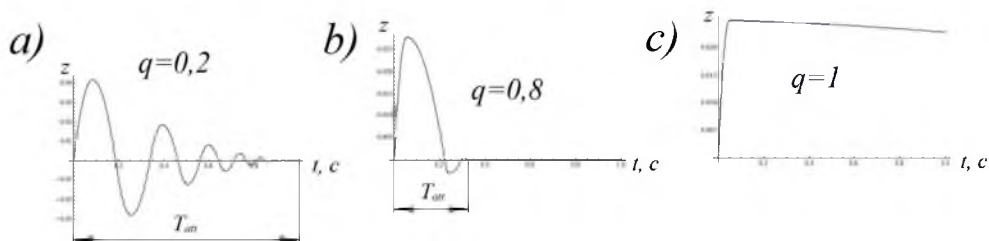


Figure 2. Simulation of damping of oscillations after an impact
 1 – elastic connections with force characteristics, shown in Fig. 1; 2 – protected object with mass m (a); b) – protected object with moment of inertia I_0 (a – linear case; b – rotational case);
 $M(\varphi)$, $F(x)$ – force characteristics, shown in Fig. 1

Results of numerical solution of the equations (1) for different values of q are presented in Fig. 3.



$z_0 = 0$; $\dot{z}_0 = 2 \text{ m/s}$; $a = 1000 \text{ kg}$; $B = 10000 \text{ N}$ - in a linear case (see Fig. 2, a);
 $\dot{z}_0 = 2 \text{ rad/s}$; $a = 1000 \text{ kg} \cdot \text{m}^2$; $B = 10000 \text{ N} \cdot \text{m}$ - in a rotational case (see Fig. 2, b);

Figure 3. Coordinate of the protected object after an impact

The differential equation, describing motion of the protected object, in case of the force characteristic shown in Fig. 1, b is the following:

$$a \cdot \ddot{z}(t) + (((q \cdot B) \cdot th[k \cdot (Abs[z(t)] - z_*)] + (q \cdot B) / 2) \cdot sign(\dot{z}(t)) + ((B \cdot th[k \cdot (Abs[z(t)] - z_*)] + B) / 2) \cdot sign(z(t))) = 0 \tag{2}$$

where z_* is the variable that describes an interval with zero force in a neutral position; $k=10000$ – the coefficient that describes rectangular shape of the hysteresis loops (Fig. 1, b).

Solution of the differential equation (2) shows that the protected object doesn't stop finally. So the criteria of a stop simulation is taken such that the velocity reduces to $0,01 \cdot V_0$. Results of the simulation of the differential equation (2) are shown in Fig. 4

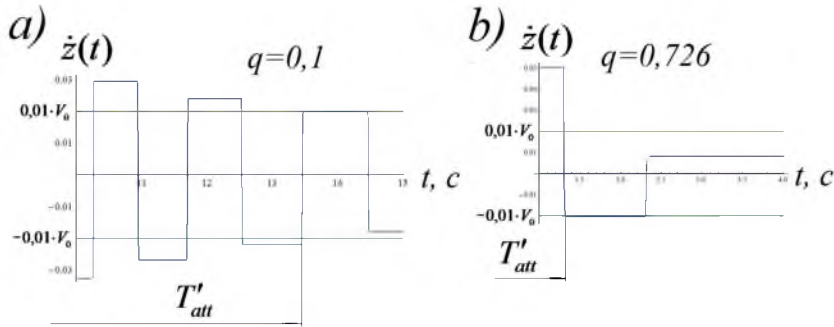


Figure 4. Dependence of velocity of the protected object with time

$z_0 = 0$; $\dot{z}_0 = 2 \text{ m/s}$; $a = 1000 \text{ kg}$; $B = 10000 \text{ N}$ - in a linear case (see Fig. 2, a);
 $\dot{z}_0 = 2 \text{ rad/s}$; $a = 1000 \text{ kg} \cdot \text{m}^2$; $B = 10000 \text{ N} \cdot \text{m}$ - in a rotational case (see Fig. 2, b);
 T'_{att} - damping time (up to $0,01 V_0$).

In [2] it was shown, that the damping time of protection systems with force characteristics presented in Fig. 1,a is the following

$$T'_{att} = \frac{a \cdot \dot{z}_0}{B} \cdot \left(\frac{2}{1+q} + \frac{1}{\sqrt{1-q^2}} + \frac{\sqrt{1-q}}{(1+q) \cdot \sqrt{1+q}} \right) \cdot \frac{1}{1-(1-q)/(1+q)} \quad (3)$$

Coefficient q is calculated when $T'_{att}(q)$ is minimized: $q_* \approx 0,786$ [2].

In Fig. 5 we present damping time relative to the coefficient q . Damping time T'_{att} is minimized when $q'_* \approx 0,980$ (it was achieved by numerical solution). It should be mentioned that q'_* doesn't depend on x_* [2]. Moreover, when q exceeds q_* (Fig. 5, a) or q'_* (Fig. 5, b), damping time greatly increases.

In Fig. 6 there are schemes of oscillating systems that provide the analyzed force characteristics $F(x)$. In Figs. 6,a and 6,b there are linear cases: elastic element moves perpendicular to the symmetry axes of the guides. Guides are described by functions $f(x)$ (Fig. 6, a) and $f_*(x)$ (Fig. 6, b) [5]. In Fig. 6,a the elastic element is compressed. In Fig. 6,b the elastic element is stretched. Note that the compressed elastic element can lose its equilibrium.

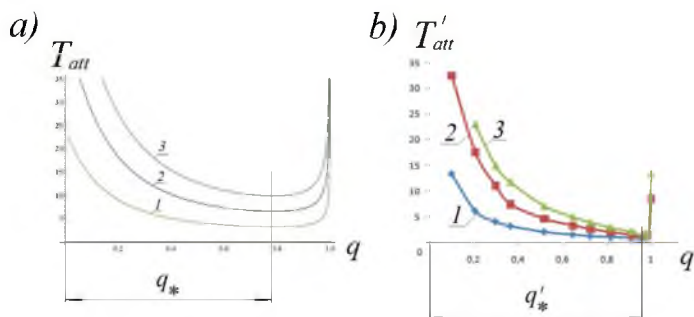
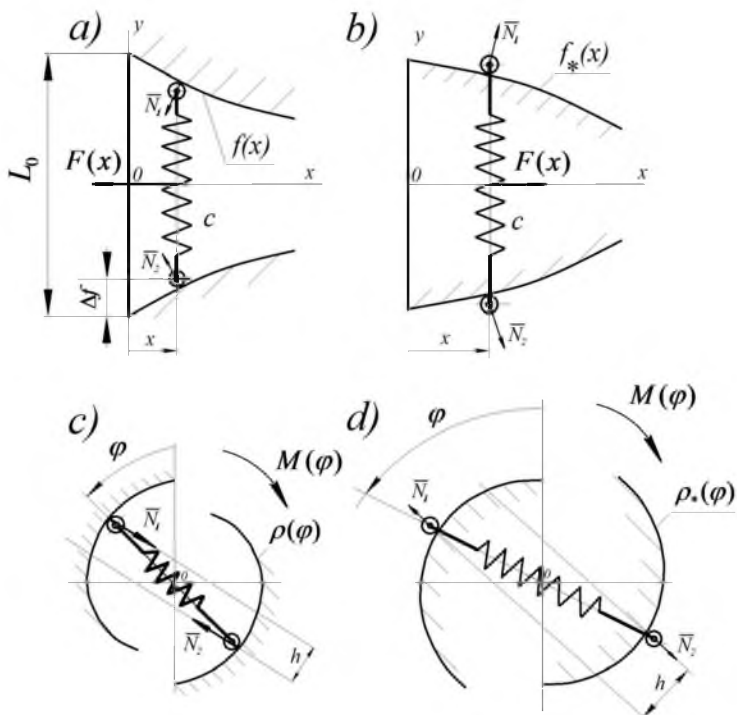


Figure 5. Damping time relative to the coefficient q

- a) 1 - $\dot{z}_0 = 3 \text{ m/s}$; 2 - $\dot{z}_0 = 2 \text{ m/s}$; 3 - $\dot{z}_0 = 1 \text{ m/s}$ - in a linear case (see Fig. 2, a);
 1 - $\dot{z}_0 = 3 \text{ s}^{-1}$; 2 - $\dot{z}_0 = 2 \text{ s}^{-1}$; 3 - $\dot{z}_0 = 1 \text{ s}^{-1}$ - in a rotational case (see Fig. 2, b);
- b) 1 - $x_* = 0,01 \text{ m}$; 2 - $x_* = 0,02 \text{ m}$; 3 - $x_* = 0,03 \text{ m}$ - in a linear case (see Fig. 2, a);
 1 - $\varphi_* = 0,01 \text{ rad}$; 2 - $\varphi_* = 0,02 \text{ rad}$; 3 - $\varphi_* = 0,03 \text{ rad}$ - in a rotational case (see Fig. 2, b);

We present the schemes of elastic hinges with analyzed angular force characteristics $M(\varphi)$ in the Figs. 6, c and Figs. 6, d. In Fig. 6, c the compressed elastic element moves between circular guides, defined by the polar coordinate $\rho(\varphi)$. In Fig. 6, d the stretched element moves between circular guides, defined by another polar coordinate $\rho_*(\varphi)$. Restoring moment $M(\varphi) = N_1 \cdot h$ is achieved by reactions N_1 and N_2 because these reactions do not pass through the center of rotation. Note that in Fig. 6 there is no mechanism for dry friction achievement required for hysteresis loops. Such mechanisms are described in [1, 3].



(a), b) – a linear case. Fig. 2, a); c), d) – a rotational case. Fig. 2, b);
 a), c) – elastic element is stretched; b), d) - elastic element is compressed).
Figure 6. Elastic systems for achieving force characteristics from the Fig. 1

Restoring force $F(x)$ for case from Fig. 6, a), b) can be calculated by the following way: (radius of rollers equals zero, initial length of spring is L_0):

$$F(x) = -\frac{\partial \Pi}{\partial x} \quad (4)$$

where $\Pi = \frac{c}{2}(L_0 - 2 \cdot f(x))^2$ – potential energy of spring with stiffness c at displacement x (at $x=0$ spring is unstressed).

One considers $F(x) = F_* \cdot \text{Tanh}[k \cdot x]$. This function is a good approximation for the force characteristic shown in Fig. 1 at big values of k . Therefore, differential equation (4) can be written as:

$$F_* \cdot \text{Tanh}[k \cdot x] = 2 \cdot c \cdot \left(\frac{df(x)}{dx}\right) \cdot (2 \cdot f(x) - L_0) \quad (5)$$

After transformations one has $\int F_* \cdot \text{Tanh}[k \cdot x] dx = 4c \int f(x) dy - 2cL_0 \int dy$. Then we get

$$F_* \ln[\text{Coshp}[k \cdot x]] / k = 4c \frac{f(x)^2}{2} - 2cL_0 f(x) + C_0, \quad (6)$$

where C_0 is a constant of integration. To obtain the value of C_0 we use the following initial parameters: $x = 0, f(x = 0) = L_0 / 2 = 0,06 \text{ m}$.

Solution of (6) leads to:

$$f(x) = \frac{L_0}{2} \pm \sqrt{F_* \cdot \ln[\text{Cosh}[k \cdot x]] / (2c \cdot k)} \quad (7)$$

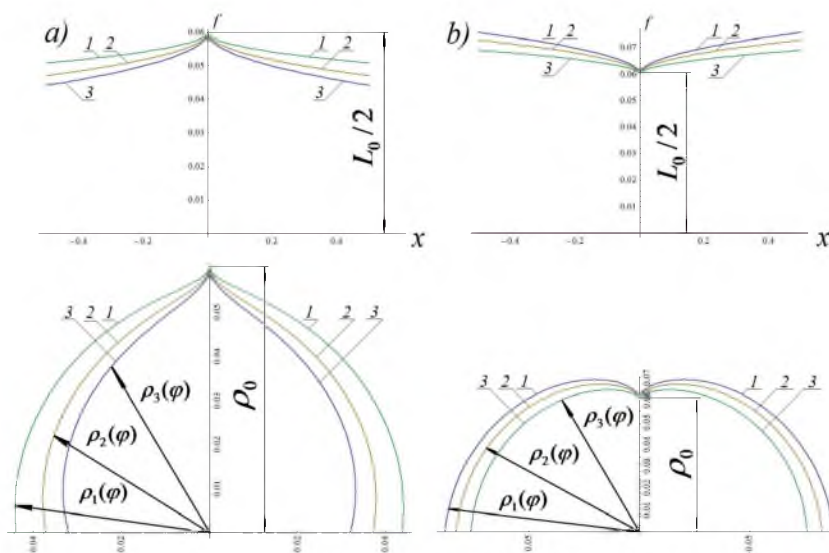
At sign «-» form of guides is concave (Fig. 6, a); at sign «+» - form of guides is convex (Fig. 6, b). Substituting $M(\varphi)$ to the force $F(x)$, one obtains the following:

$$\rho(\varphi) = \frac{L_0}{2} \pm \sqrt{M_* \cdot \ln[\text{Cosh}[k \cdot \varphi]] / (2c \cdot k)}. \quad (8)$$

There are forms of guides described in Fig. 7 by the formulas (7) (top Figs.) and (8) (lower Figs.). In Fig. 7, a) the formulas (7) and (8) have sign «minus»; in Fig. 7, b) the formulas (7) and (8) have sign «plus». The radius of rollers equals zero. If the radius does not equal zero, it is necessary to construct equidistant guides. Example of an analytical construction of these guides is presented in [6].

Conclusions

Oscillations of the systems with force characteristics with hysteresis loops of rectangular shape obtained by dry friction forces are analyzed. Such a force characteristic can be achieved by special guides. Methods of calculation of the guides are presented. Linear and rotary cases of the system were analyzed. Optimal dimensions of hysteresis loops were calculated for minimum damping of oscillation. The analyzed systems can be used in different fields of Engineering: seismic protection, chassis of transport, exoskeletons.



1 - $c = 3 \cdot 10^7$ N/m; 2 - $c = 1,5 \cdot 10^7$ N/m; 3 - $c = 10^7$ N/m

Figure 7. Guides for achieving force characteristics defined by $F(x) = F_0 \cdot \text{Tanh}[k \cdot x]$ ($M(\varphi) = M_0 \cdot \text{Tanh}[k \cdot \varphi]$, see Fig. 1, a).

References

- [1] Zotov A.N. Systems with quasi-zero-stiffness characteristic. In: *Proceeding of the 6th EUROMECH Nonlinear Dynamics Conference, ENOC 2008*. Saint Petersburg, 2008.
- [2] Zotov A.N., Valeev A.R. and Tikhonov A.Yu. The vibroprotective and impactprotective systems which have force characteristics with rectangular loops of hysteresis. *Izvestia Vischich Uchebnich Zavedeney*, N1, 2010.
- [3] Valeev A.R. and Zotov A.N. *Protection against impact and vibration systems with quasi-zero stiffness*. Neftgazovoye dcllo, Ufa, 2013.
- [4] Zotov A.N. Oscillation of systems which have force-displacement characteristics with rectangular loops of hysteresis. In: *ND-KhPI2010: Proceeding of the 3th Int. Conf. on Nonlinear Dynamics, September 19-24, 2010*. Kharkov, 2010.
- [5] Tchelomei V.N. *Vibrations in equipment*. Mashinostroyeniye, Moscow, 1978.
- [6] Zotov A.N. Elastic joints with given force characteristics. In: *Materials of the All-Russian scientific and technical conference "Mathematical Modelling of the Mechanical Phenomena", May 17-18, 2013*. Yekaterinburg, pp. 61-65, 2013.